Lown, J. W., Majumdar, K. C., Meyers, A. I., & Hecht, A. (1977) *Bioorg. Chem. 6*, 453-463.
Lown, J. W., Sim, S. K., & Chen, H. H. (1978) *Can. J. Biochem. 56*, 1042-1047.
Lown, J. W., Chen, H. H., Plambeck, J. A., & Acton, E. M. (1979) *Biochem. Pharmacol. 28*, 2563-2568.
Lown, J. W., Joshua, A. V., & Chen, H. H. (1981) *Can. J. Chem. 59*, 2945-2952.
Mahler, H. R., & Cordes, E. H. (1966) *Biological Chemistry*, p 207, Harper and Row, New York.
McChee, J. D. (1976) *Biopolymers 15*, 1345-1375.
McClune, G. J., & Fee, J. A. (1976) *FEBS Lett. 67*, 294-298.
Morgan, A. R., & Paetkau, V. (1972) *Can. J. Biochem. 50*, 210-216.
Morgan, A. R., & Pulleyblank, D. E. (1974) *Biochem. Biophys. Res. Commun. 61*, 396-403.
Morgan, A. R., Lee, J. S., Pulleyblank, D. E., Murray, N. L., & Evans, D. H. (1979) *Nucleic Acids Res. 7*, 547-569.
Rao, K. V., Biemann, K., & Woodward, R. B. (1963) *J. Am. Chem. Soc. 85*, 2532-2533.
Rao, G. M., Begleiter, A., Lown, J. W., & Plambeck, J. A. (1977) *J. Electrochem. Soc. 124*, 199-202.
Rao, G. M., Lown, J. W., & Plambeck, J. A. (1978) *J. Electrochem. Soc. 125*, 534-539.
Sausville, E. A., Peisach, J., & Horwitz, S. B. (1976) *Biochem. Biophys. Res. Commun. 73*, 814-822.
Szybalski, W., & Iyer, V. N. (1967) in *The Mitomycins and Porfiromycins* in *Antibiotics 1. Mechanism of Action* (Gottlieb, D., & Shaw, P. D., Eds.) pp 211-245, Springer-Verlag, New York.
van Hemmen, J. J., & Meuling, W. J. S. (1977) *Arch. Biochem. Biophys. 182*, 743-748.

Premelting and Melting Transitions in the d(CGCGAATTCGCG) Self-Complementary Duplex in Solution†

Dinshaw J. Patel,* Sharon A. Kozlowski, Luis A. Marky, Chris Broka, Janet A. Rice, Keiichi Itakura, and Kenneth J. Breslauer

ABSTRACT: We have characterized structural and dynamic aspects of the d($C_1G_2C_3G_4A_5A_6T_6T_5C_4G_3C_2G_1$) 12-mer duplex based on an analysis of the proton and phosphorus nuclear magnetic resonance parameters in the premelting and melting transition region. The self-complementary dodecanucleotide sequence forms a 12 base-paired duplex with 2-fold symmetry in solution. The six Watson–Crick imino protons are well resolved between 12.5 and 14.0 ppm and have been assigned to individual positions in the sequence. Fraying of the ends of the duplex is most pronounced at terminal base pair 1. This fraying extends into the interior of the duplex up to and including base pair 3 with increasing temperature in the premelting transition region. A temperature-dependent transition is detected in the dA·dT-containing tetranucleotide core of the duplex in the premelting temperature range, which is not observed at the flanking dG·dC-containing tetranucleotide regions. The 11 phosphodiesters in the 12-mer duplex exhibit ^{31}P chemical shifts spread over a 0.45-ppm chemical shift range, suggestive of a distribution of O–P torsion angles and/or O–P–O bond angles at individual phosphodiester linkages along the sequence. Well-resolved resonances of nonexchangeable base protons are observed in the 12-mer duplex spectrum. Partial assignment of these resonances to specific base pairs in the 12-mer was accomplished with spin decoupling, nuclear Overhauser effect, and chemical modification studies. These base protons shift as average resonances during the helix–coil transition of the 12-mer duplex in 0.1 M phosphate solution with a transition midpoint of 72 ± 2 °C at the 10 nonterminal base pairs. Upfield shifts are observed at the base protons of the dodecanucleotide sequence on duplex formation, which reflect the stacking interactions in the double-helical state. The thermally induced transitions of the right-handed 12-mer duplex in 0.01 and 0.1 M NaCl were investigated by differential scanning calorimetry. In 0.01 M NaCl an enthalpy change of 90 kcal (mol of double strand)$^{-1}$ was measured with a melting temperature of 65.5 °C. In 0.1 M NaCl an enthalpy change of 102 kcal (mol of double strand)$^{-1}$ was measured with a melting temperature of 71.3 °C. Analysis of the shapes of the calorimetric heat capacity curves yields van't Hoff enthalpies of 94 kcal in 0.01 M NaCl and 74 kcal in 0.1 M NaCl. Thus, we conclude that in 0.01 M NaCl the transition approaches two-state behavior ($\Delta H_{cal} = \Delta H_{V.H.}$) while in 0.1 M NaCl the transition from duplex to strands involves intermediate states ($\Delta H_{V.H.} < \Delta H_{cal}$). The ratio of the van't Hoff and calorimetric enthalpies allows specification of the size of the cooperative unit. Thus, in 0.1 M NaCl 9 ± 1 base pairs of the 12-mer melt in a cooperative manner.

We have begun a program in which nuclear magnetic resonance (NMR) and differential scanning calorimetry (DSC) have been used to investigate the conformation, dynamics, and thermodynamics of order–disorder transitions in a series of DNA duplexes containing at least one turn of helix in which the structures systematically differ due to selected modifications.

Our initial studies focused on the self-complementary dodecanucleotide d(CGCGAATTCGCG) duplex (Chart I) since parallel crystallographic investigations have been undertaken (Wing et al., 1980; Drew et al., 1981; Dickerson & Drew, 1981) and should permit a direct comparison between data obtained in solution with that obtained at atomic resolution in the crystalline state.

The application of high-resolution nuclear magnetic reso-

† From Bell Laboratories, Inc., Murray Hill, New Jersey 07974 (D.J.P., S.A.K., and J.A.R.), the Department of Chemistry, Douglass College, Rutgers University, New Brunswick, New Jersey 08903 (L.A.M. and K.J.B.), and the City of Hope National Medical Center, Duarte, California 91010 (C.B. and K.I.). *Received May 22, 1981; revised manuscript received September 3, 1981.* K.J.B. and L.A.M. gratefully acknowledge support from the National Institutes of Health, Grant GM-23509, the Research Corporation, and the Charles and Johanna Busch Memorial Fund.

0006-2960/82/0421-0428$01.25/0

Chart I

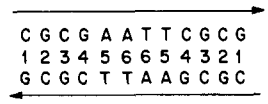

Scheme I: Synthesis of d(CGCGAATTCGCG)

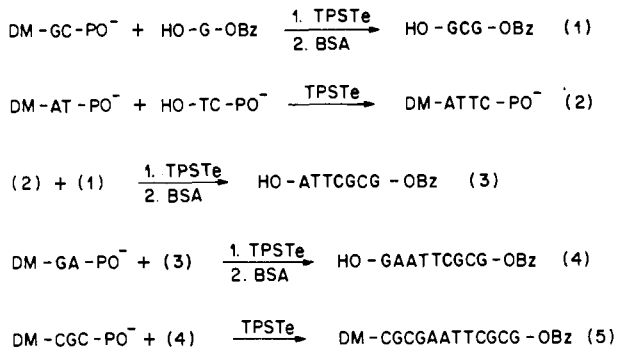

nance spectroscopy toward the elucidation of structural features of helix to coil transitions in deoxyoligonucleotide duplexes is well documented at the complementary and self-complementary oligonucleotide and synthetic DNA level (Cross & Crothers, 1971; Crothers et al., 1973; Patel 1974, 1979, 1980; Kallenbach et al., 1976; Early et al., 1977, 1980; Selsing et al., 1978; Patel & Canuel, 1979; Haasnoot et al., 1980; Miller et al., 1980; Schweizer, 1980; Pardi et al., 1981).

Differential scanning calorimetry of order–disorder transitions in oligonucleotide duplexes can provide the basis for a complete thermodynamic characterization of the molecular forces that control the structure and conformational flexibility of nucleic acids in solution (Breslauer et al., 1975; Albergo et al., 1981; Marky et al., 1981).

This paper describes high-resolution NMR and DSC studies of the premelting and melting transitions of the d-(CGCGAATTCGCG) 12-mer duplex in aqueous solution.

Experimental Procedures

Synthesis. The dodecanucleotide was prepared by the modified triester method (Hirose et al., 1978) as outlined in Scheme I.

General Coupling Procedure. An oligonucleotide (1.5 equiv) protected at the 5′ end with a 4,4-dimethyltrityl group (DM) and containing a reactive *o*-chlorophenyl phosphate (PO^-) at the 3′ end plus 1 equiv of an oligonucleotide containing a free hydroxyl group (HO) at the 5′ end and a benzoyl group (OBz) at the 3′ end are taken up in pyridine and evacuated in vacuo. The procedure is repeated to ensure freedom from moisture, and 2–2.5 equiv of 2,4,6-triisopropylbenzenesulfonyl tetrazolide (TPSTe) is added to a concentrated solution of the reactants in pyridine (1.5 mL/mmol). The reaction is completed in less than 3 h as monitored by silica gel thin-layer chromatography (TLC). The reaction is stopped by addition of water and the solution evaporated in vacuo. The product is taken up in chloroform, washed repeatedly with 5% sodium bicarbonate, and with water, dried over $MgSO_4$, and evaporated in vacuo with a little toluene to azeotrope off residual pyridine. The protected oligonucleotide is purified by silica gel chromatography with a 0–4–6% methanol gradient in chloroform. The DM–oligonucleotide–OBz product is deprotected at the 5′ end with benzenesulfonic acid (BSE) to yield the HO–oligonucleotide–OBz to be used in subsequent coupling steps. The bases are N-benzoylated at adenine and cytosine and N-isobutyrylated at guanine during the coupling reactions.

Preparation of HO–GCG–OBz (1). HO–G–OBz (0.66 g, 1.5 mmol) and 3.0 g of DM–GC–PO^- (2.5 mmol) were condensed in the presence of 1 g of TPSTe in dry pyridine (1.5 mL/mmol). Workup and silica gel chromatography (gradient of methanol in chloroform) afforded pure DM–GCG–OBz in 78% yield. Deprotection with 2% BSE in 3:7 methanol/chloroform at 5 °C for 5 min followed by washing with saturated sodium bicarbonate, drying, concentration, and trituration (1:2 ethyl ether/pentane) gave HO–GCG–OBz (1).

Preparation of DM–ATTC–PO⁻ (2). DM–AT–PCE (3.9 g, 3 mmol) was deblocked (1:1:3 triethylamine/water/pyridine, 20 °C, 15 min) and condensed with 1.95 g of HO–TC–PCE (2 mmol) in the presence of 1.3 g of TPSTe. Following workup and purification, DM–ATTC–PO^- (2) was isolated in 82% yield.

Preparation of HO–ATTCGCG–OBz (3). DM–ATTC–PCE (3.77 g, 1.77 mmol) was deblocked as before and condensed with 1.60 g of HO–GCG–OBz (1.11 mmol) in the presence of TPSTe condensing agent. The product was detritylated with BSE and chromatographed to yield the 7-mer HO–ATTCGCG–OBz (3).

Preparation of HO–GAATTCGCG–OBz (4). The 7-mer HO–ATTCGCG–OBz was condensed with 1.5 equiv of DM–GA–PO^- to give the protected 9-mer DM–GAATTCGCG–OBz in 60% yield, based on HO–GCG–OBz. Detritylation yielded HO–GAATTCGCG–OBz (4), which was used for the synthesis of the various dodecanucleotide duplexes outlined in this and subsequent papers in this series.

Preparation of DM–CGCGAATTCGCG–OBz (5). HO-GAATTCGCG-OBz (0.35 g, 0.08 mmol) was condensed with 0.224 g of DM–CGC–PO^- (0.12 mmol) in the presence of TPSTe condensing agent. The product was worked up and chromatographed through a short column of silica gel to yield 82% of fully protected DM–CGCGAATTCGCG–OBz (5).

Deprotection and Purification of Dodecamer. The *o*-chlorophenyl and base-protecting groups were removed by heating overnight at 50 °C in 1:1 concentrated ammonium hydroxide/pyridine in a closed flask. The basic reaction medium was removed under vacuum and the product dried prior to treatment with 80% acetic acid for 20 min. The acid was removed under vacuum, and the product was taken up in aqueous solution and washed repeatedly with ether to remove the trityl alcohol and other byproducts. The deprotected 12-mer in aqueous solution was passed through a millipore filter, and 8000 OD units of 12-mer was taken up in 500 mL of 7 M urea, 0.2 M KCl, and 0.05 M Tris[1] buffer, pH 7.5. This was applied to a 50 cm × 1.5 cm column of DE-23, which was eluted with a salt gradient ranging from 0.2 to 0.4 M KCl. A sharp peak containing 950 OD units was collected and reapplied following a 7-fold dilution to a 6-cm DE-23 ion-exchange column. The urea and salts were removed by elution with excess 5 mM triethylammonium bicarbonate buffer, pH 7.8. The dodecanucleotide was eluted with 1 M triethylammonium bicarbonate and the salt removed by evaporation under vacuum.

NMR Spectra. The exchangeable protons of the dodecanucleotide in H_2O were recorded in the correlation mode on a Bruker WH-360 spectrometer with 1-s acquisition time per scan. The nuclear Overhauser effect (NOE) experiments on the 12-mer duplex in H_2O solution were recorded on a Nicolet 360-MHz spectrometer with the application of a Redfield 214 low-power pulse sequence to null the H_2O resonance. The temperature-dependent nonexchangeable proton spectra of the dodecanucleotide duplex were recorded in the Fourier trans-

[1] Abbreviations: OD, optical density; Tris, tris(hydroxymethyl)-aminomethane; EDTA, ethylenediaminetetraacetic acid.

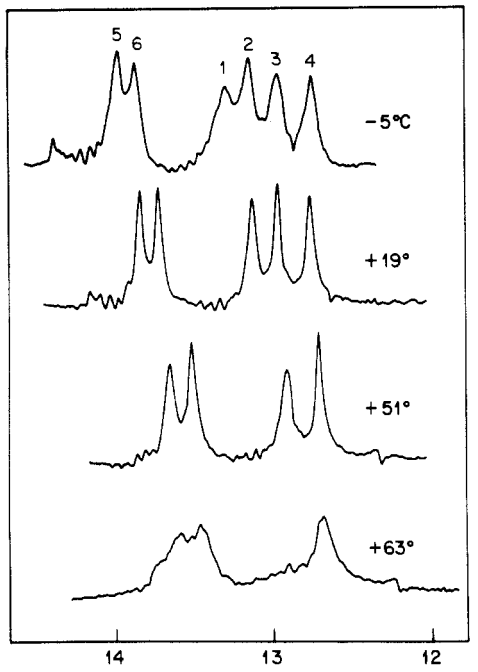

FIGURE 1: The 360-MHz correlation proton NMR spectra (12–14 ppm) of the 12-mer duplex in 0.1 M phosphate, 2.5 mM EDTA, and 4:1 $H_2O/^2H_2O$, pH 7.50, between −5 and +63 °C. The signal to noise of the spectra was improved by applying a 5-Hz exponential line broadening contribution.

form mode on an HX-360 NMR spectrometer. A proton spectrum of the 12-mer duplex in ^2H_2O at ambient temperature was recorded on the Caltech 500-MHz spectrometer. The spin decoupling experiments were undertaken in the Fourier transform mode on a WH-500 spectrometer. The chemical shifts are referenced relative to the internal standard 4,4-dimethyl-4-silapentanesulfonate (DSS).

The dodecanucleotide 81-MHz phosphorus NMR spectra were recorded with broad band proton noise decoupling on a Varian XL-200 spectrometer in the Fourier transform mode. The chemical shifts are referenced relative to the internal standard trimethyl phosphate. Phosphorus spin–lattice relaxation times were measured by the inversion recovery method under conditions of broad band proton decoupling. The data were accumulated in the interleave mode with a 10-s repetition rate between pulses. Phosphorus nuclear Overhauser effects were measured with the gated decoupling technique. Data were accumulated in the interleave mode with the broad band decoupler either on or off during the 10-s repetition rate between pulses.

Calorimetry. The differential scanning calorimetry was carried out on a Microcal-1 instrument similar to one previously described in detail (Jackson & Brandts, 1970). In a typical experiment, the reaction and the reference platinum cells are each filled with 0.9 mL of solution, and the temperature is scanned from 5 to 95 °C at a rate of 0.94 °C/min. For a thermally induced endothermic transition, the temperature of the reaction cell will lag behind that of the solvent reference cell. In a given experiment, one continuously measures the additional electrical energy fed back to the reaction cell to maintain it at the same temperature as the solvent reference cell. The instrument is calibrated by measuring the area produced by a controlled electrical pulse. These data (along with the known concentration of the solute) permit the construction of a specific heat vs. temperature curve. The data are plotted as excess heat capacity values relative to buffer. The concentration of the 12-mer for the calorimetric measurements is based on an extinction coefficient of 1.15×10^5 in strands at 90 °C and 260 nm.

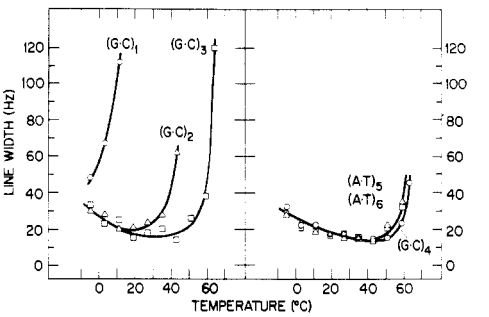

FIGURE 2: The temperature dependence of the line widths of the six imino protons of the 12-mer duplex in 0.1 M phosphate, 2.5 mM EDTA, and 4:1 $H_2O/^2H_2O$, pH 7.50, between −5 and +63 °C.

Table I: Assignment of the Imino Watson-Crick Proton Chemical Shift to Individual Base Pairs in the 12-mer Duplex at −5 °C[a]

base pair	assignment	chemical shift (ppm)
dG·dC	1	13.29
dG·dC	2	13.14
dG·dC	3	12.96
dG·dC	4	12.75
dA·dT	5	13.97
dA·dT	6	13.86

[a] Buffer: 0.1 M phosphate, 2.5 mM EDTA, and 4:1 $H_2O/^2H_2O$, pH 7.50.

Results

NMR Studies. The d(CGCGAATTCGCG) duplex exhibits 2-fold symmetry, and the base pairs are numbered 1–6 proceeding from the ends to the interior of the double helix (Chart I).

(A) Imino Proton Spectra. The 360-MHz proton correlation NMR spectra (12–14 ppm) of the 12-mer duplex in 0.1 M phosphate and H_2O, pH 7.5, between −5 and +63 °C are presented in Figure 1. We observe six resonances corresponding to the six base pairs related by 2-fold symmetry in the −5 °C dodecanucleotide spectrum (Figure 1). Previous studies on model systems (Crothers et al., 1973; Patel & Tonelli, 1974; Kallenbach et al., 1976) and transfer RNA (Patel 1978; Robillard & Reid, 1979) demonstrate that the two resonances at low field correspond to the thymidine H-3 imino proton in dA·dT base pairs while the four resonances at high field correspond to the guanosine H-1 imino proton in dG·dC base pairs for the −5 °C spectrum of the 12-mer duplex (Figure 1).

(B) Imino Proton Line Widths. There is sequential broadening of guanosine H-1 imino protons at 13.29, 13.14, and 12.96 ppm of the 12-mer duplex on raising the temperature from −5 to +60 °C in 0.1 M phosphate, pH 7.5 solution (Figure 1). The remaining guanosine H-1 imino proton at ~12.7 ppm and the two thymidine imino protons at ~13.5 ppm in the 12-mer duplex broaden to the same extent above 60 °C (Figure 1). The temperature-dependent line widths of the 12-mer duplex in 0.1 M phosphate, pH 7.5, between −5 and +63 °C are plotted in Figure 2.

(C) Guanosine Imino Proton Assignments. The observed sequential broadening of the guanosine imino protons originates in fraying at the ends of the duplex (Patel, 1974; Patel & Hilbers, 1975; Kan et al., 1975) and permits the assignment of the 13.29, 13.14, 12.96, and 12.75 ppm resonances to the imino protons of dG·dC base pairs at positions 1, 2, 3, and 4, respectively, at −5 °C (Table I).

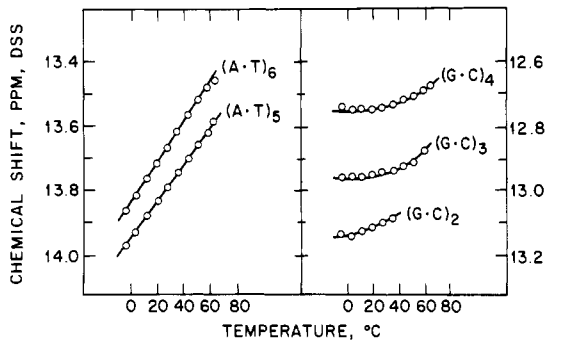

FIGURE 3: The temperature dependence of the chemical shifts of the six imino protons of the 12-mer duplex in 0.1 M phosphate, 2.5 mM EDTA, and 4:1 $H_2O/^2H_2O$, pH 7.50, between −5 and +63 °C.

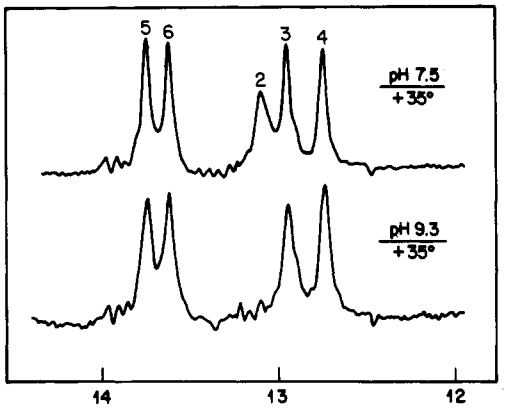

FIGURE 4: The 360-MHz correlation proton NMR spectra (12–14 ppm) of the 12-mer duplex in 0.1 M phosphate, 2.5 mM EDTA, and 4:1 $H_2O/^2H_2O$, 35 °C, at pH 7.5 and 9.3. The signal to noise of the spectra was improved by applying a 5-Hz exponential line broadening contribution.

(D) Thymidine Imino Proton Assignments. We have assigned (see NOE studies in a later section) the downfield imino proton at 13.97 ppm to dA·dT base pair 5 and the upfield imino proton at 13.86 ppm to dA·dT base pair 6 in the 12-mer duplex at −5 °C (Table I, Figure 1).

(E) Imino Proton Chemical Shifts. The temperature-dependent chemical shifts of the six imino protons in the 12-mer duplex are plotted between −5 and +63 °C in Figure 3. Since the data for terminal dG·dC base pair 1 are limited to one temperature, we focus on the remaining five base pairs. We observe a small upfield shift (<0.1 ppm) for the guanosine H-1 protons at base pairs 2–4 over this temperature range. Specifically, the imino protons of base pairs 3 and 4 exhibit temperature-independent chemical shifts between −5 and +30 °C (Figure 3).

By striking contrast, the thymidine H-3 protons of base pairs 5 and 6 of the 12-mer duplex shift ~0.4 ppm to high field on raising the temperature from −5 to +63 °C (Figure 3). The chemical shift change at these resonances in the center of the dodecamer duplex are linear with temperature and of similar magnitude.

(F) Base Catalysis of Exchange. The imino protons in the dodecanucleotide duplex broadened in the order: base pair 1 followed by 2 and then 3 with base pairs 4–6 broadening out simultaneously with increasing temperature (Figures 1 and 2).

The pH dependence of the imino proton spectra of the 12-mer duplex at 35 °C is presented in Figure 4, and it can be readily noted that the guanosine H-1 imino proton of base pair 2 at ~13.1 ppm in the pH 7.5 spectrum is completely broadened out in the pH 9.3 spectrum. The effect of pH on the line widths of the 12-mer as a function of temperature is most pronounced at base pair 1, decreases at base pair 2, and decreases further at base pair 3.

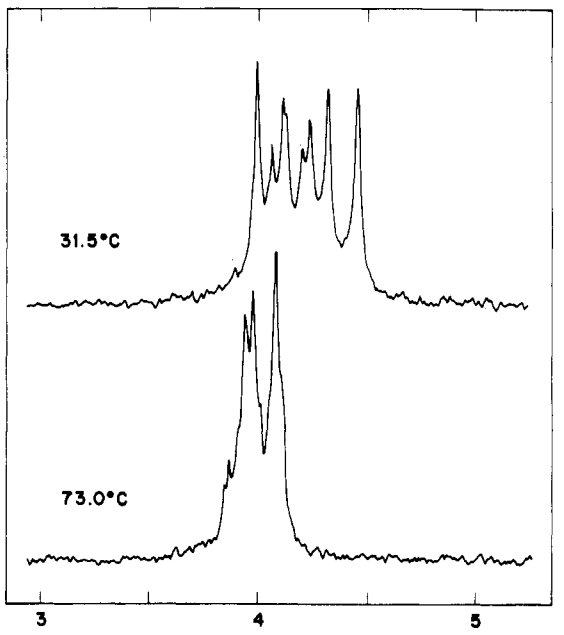

FIGURE 5: The proton noise decoupled 80.995-MHz Fourier transform phosphorus NMR spectra (3–5 ppm upfield from standard trimethyl phosphate) of the 12-mer in 20 mM phosphate, 0.5 mM EDTA, and ^2H_2O, pH 8.0, at 31.5 and 73.0 °C. The signal to noise of the spectra was improved by applying a 0.5-Hz exponential line broadening contribution. The chemical shifts are not corrected for the temperature dependence of the standard.

Table II: 81-MHz ^{31}P Spin-Lattice Relaxation Time (T_1) and Nuclear Overhauser Effect ($1 + \eta$) for the Resolved Phosphodiesters in the 12-mer Duplex at 20 °C[a]

chemical shift (ppm)[b]	area	relaxation time, T_1 (s)[c]	NOE $(1 + \eta)$[d]
4.013	2	1.55	1.12
4.055[e]	1	1.66	0.96
4.151	2	1.62	1.11
4.258	2	1.81	1.05
4.367	2	1.62	1.04
4.479	2	1.53	1.03

[a] Buffer: 20 mM phosphate, 0.5 mM EDTA, and ^2H_2O, pH 8.0. [b] Upfield from internal standard trimethyl phosphate. [c] T_1 values measured by interleaved inversion recovery method with a repetition delay of 10 s. [d] NOE values measured by interleaved gated decoupling method with a repetition delay of 10 s. [e] Shoulder on 4.013 ppm resonance.

(G) Phosphorus Spectra. Proton noise decoupled 81-MHz ^{31}P spectra of the 12-mer duplex in 20 mM phosphate solution at 31.5 and 73.0 °C are presented in Figure 5. In the duplex state at 31.5 °C, eight partially resolved spread over a 0.45 ppm chemical shift range are observed. By contrast, in the strand state at 73.0 °C the chemical shifts are spread over 0.25 ppm (Figure 5). At this time we are unable to assign the resolved phosphorus resonances to specific phosphodiesters in the d(CGCGAATTCGCG) sequence.

We have evaluated the 81-MHz ^{31}P spin–lattice relaxation times (T_1) and the $^{31}P[^1H]$ nuclear Overhauser effect ($1 + \eta$) for the resolved phosphodiesters in the 12-mer spectrum at 20 °C (Table II). The T_1 relaxation time values range between 1.5 and 1.8 s while the $1 + \eta$ NOE values range between 0.95 and 1.12 for the six resolved resonance in the spectrum (Table II). Thus, there are no significant differences between the T_1 and NOE values amongst the resolved phosphodiesters in the 12-mer duplex in solution at 20 °C.

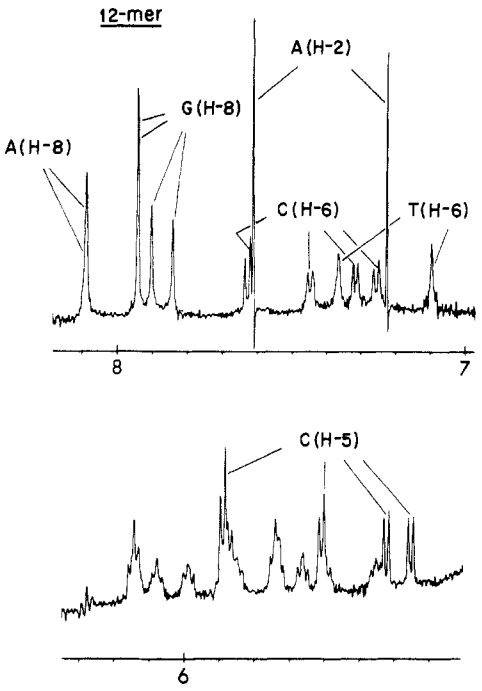

FIGURE 6: The 500-MHz Fourier transform proton NMR spectra (5.3–8.1 ppm) of the 12-mer duplex in 0.1 M phosphate, 2.5 mM EDTA, and ^2H_2O, pH 7.70, at ambient temperature. The resolution of the spectrum was improved by applying an exponential line narrowing contribution.

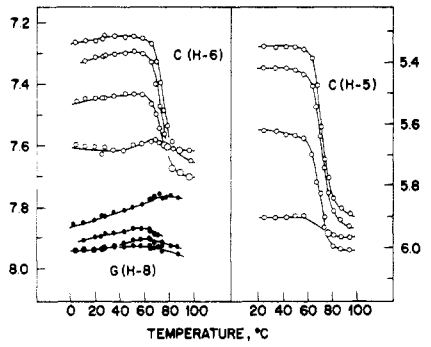

FIGURE 7: The temperature-dependent 360-MHz chemical shifts of the guanosine H-8 and the cytidine H-6 and H-5 resonances of the 12-mer duplex in 0.1 M phosphate, 2.5 mM EDTA, and ^2H_2O, pH 7.70.

(H) Nonexchangeable Proton Spectra. The 500-MHz proton NMR spectrum of the aromatic region (5.3 to 8.1 ppm) of the d(CGCGAATTCGCG) duplex in 0.1 M phosphate and ^2H_2O, pH 7.70, at ambient temperature is presented in Figure 6.

The purine H-8 resonances are deuterated at high temperature and, hence, readily distinguishable from the other resonances. The guanosine H-8 resonances are deuterated more readily than their adenosine H-8 counterparts. The two adenosine H-8 singlets are superimposed at 8.08 ppm while the four guanosine H-8 singlets resonate between 7.82 and 7.94 ppm (Figure 6).

The narrow (long relaxation time) adenosine H-2 singlets at 7.26 and 7.62 ppm can be differentiated from the broad (long-range coupling to the CH_3-5 group) thymidine H-6 singlets at 7.08 and 7.36 ppm (Figure 6).

The four cytidine H-6 doublets resonate between 7.24 and 7.62 ppm while the four cytidine H-5 doublets are observed at 5.90 ppm and between 5.35 and 5.62 ppm (Figure 6). Finally, the twelve sugar H-1′ multiplets resonate between 5.4 and 6.2 ppm (Figure 6).

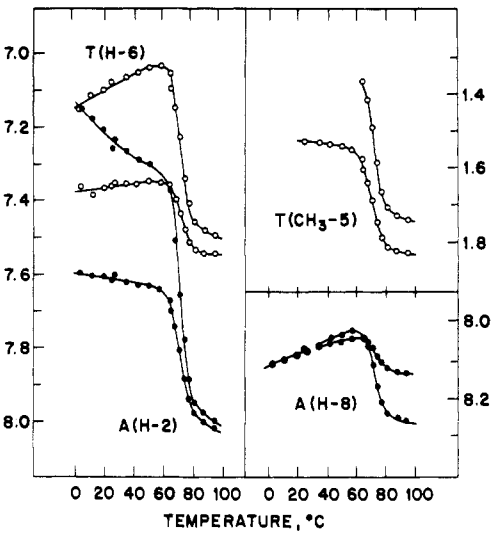

FIGURE 8: The temperature-dependent 360-MHz chemical shifts of the thymidine H-6 and CH_3-5 protons and the adenosine H-2 and H-8 protons in the 12-mer duplex in 0.1 M phosphate, 2.5 mM EDTA, and ^2H_2O, pH 7.70.

Table III: Chemical Shift of dG·dC Base Pair Nonexchangeable Protons in the 12-mer Duplex at 50 and 95 °C and Their Transition Midpoints[a]

resonance	assignment	chemical shift (ppm) 50 °C	95 °C	T_m (°C)
G(H-8)		7.93	7.94	
G(H-8)		7.91	7.94	
G(H-8)		7.87	7.94	
G(H-8)		7.80	7.77	
C(H-6)	1	7.60	7.62	
C(H-6)	4	7.43	7.70	72.0
C(H-6)	2,3	7.295	7.70	72.0
C(H-6)	2,3	7.24	7.65	74.0
C(H-5)	1	5.90	5.97	
C(H-5)	4	5.64	6.01	70.0
C(H-5)	2,3	5.43	5.94	71.5
C(H-5)	2,3	5.35	5.90	72.0

[a] Buffer: 0.1 M phosphate, 2.5 mM EDTA, and ^2H_2O, pH 7.70.

Table IV: Chemical Shift of dA·dT Base Pair Nonexchangeable Protons in the 12-mer Duplex at 50 and 95 °C and Their Transition Midpoints[a]

resonance	assignment	chemical shift (ppm) 50 °C	95 °C	T_m (°C)
A(H-8)		8.04	8.14	
A(H-8)		8.04	8.27	
A(H-2)	5	7.30	8.02	71.5
A(H-2)	6	7.63	8.00	71.5
T(H-6)	5	7.35	7.545	71.5
T(H-6)	6	7.04	7.50	72.0
T(CH_3-5)	5	1.545	1.835	70.5
T(CH_3-5)	6	~1.28	1.745	

[a] Buffer: 0.1 M phosphate, 2.5 mM EDTA, and ^2H_2O, pH 7.70.

(I) Duplex to Strand Transition. The nonexchangeable resonances of the 12-mer duplex in 0.1 M phosphate can be monitored through the duplex to strand transition as average resonances. The data for the four dG·dC base pairs are plotted in Figure 7 and for the two dA·dT base pairs are plotted in Figure 8. Those resonances, which shift by ≥0.4 ppm during the melting transition, exhibit broadening in the vicinity of the midpoint of the transition.

The nonterminal base pair resonances exhibit transition midpoints of 72 ± 2 °C for the dodecanucleotide duplex in

0.1 M phosphate with no significant differences between the three nonterminal dG·dC base pairs (Table III) and the central dA·dT base pairs (Table IV).

We attempt below to assign as many of the base protons to specific residues in the sequence. By contrast, we are unable at this time to assign any of the sugars H-1′ resonances.

(*J*) *Cytidine Proton Assignments.* The H-6 and H-5 protons on a given cytidine are coupled to each other and can be identified by spin decoupling experiments. This permitted correlation of the cytidine H-6 and H-5 protons corresponding to each of the four cytidines in the dodecanucleotide sequence. The results of the decoupling experiments are summarized in Table III.

The cytidine H-6 and H-5 resonances at lowest field, which do not exhibit significant chemical shift change during the melting transition (Figure 7, Table III), are assigned to the cytidine at position 1 in the sequence. This reflects the negligible shielding contributions from base pair 2 at this terminal residue.

The cytidines at positions 2 and 3 are located in the interior of the alternating d(CGCG) tetranucleotide segment in the dodecanucleotide duplex. It follows that the cytidine H-5 and H-6 chemical shifts at positions 2 and 3 in the dodecanucleotide should be similar to the cytidine H-5 chemical shift of ~7.28 ppm and cytidine H-6 chemical shift of ~5.38 ppm in the $(dC–dG)_n$ duplex (Patel, 1980). This permits the assignment of the two H-5 doublets at highest field and the two H-6 doublets at highest field to the cytidines at positions 2 and 3 in the dodecanucleotide sequence although we cannot distinguish between them (Table III). The remaining cytidine residue with H-6 and H-5 duplex chemical shifts at 7.43 and 5.64 ppm, respectively, are assigned to cytidine 4 in the dodecanucleotide sequence (Table III).

The cytidine H-6 and H-5 proton assignments of base pairs 1 and 4 were confirmed by NMR studies on the 4-Br^{5}dC 12-mer and 1-Br^{5}dC 12-mer analogues. Three cytidine H-6 doublets and three cytidine H-5 doublets are observed in these spectra. The missing cytidine H-6 doublet and H-5 doublet are assigned to the cytidine at the bromination site. These results unambiguously confirm the tentative assignments discussed above of the cytidine protons at positions 1 and 4 in the 12-mer duplex (Table III).

(*K*) *Guanosine Proton Assignments.* The four guanosine H-8 protons can be resolved from each other and undergo negligible shifts during the 12-mer duplex to strand transition (Figure 7). Currently, we are unable to assign individual H-8 resonances to specific guanosines in the sequence.

(*L*) *Thymidine Proton Assignments.* The d(GGAATTCC) 8-mer duplex and the d(CGCGAATTCGCG) 12-mer duplex have a common d(GAATTC) hexanucleotide core. This results in the thymidine base proton resonances exhibiting similar chemical shifts in the 8-mer and 12-mer duplexes. We have distinguished between the two thymidines in the d(GGAATTC) duplex by studies on an analogue where one of the dT residues is replaced by a trifluoromethyl^{5}dU residue (D. J. Patel, C. Broka, and K. Itakura, unpublished results). The known thymidine assignments in the 8-mer duplex permits by analogy the assignment of the downfield thymidine H-6 and CH_3-5 to position 5 and the upfield thymidine H-6 and CH_3-5 to position 6 in the 12-mer duplex (Table IV).

(*M*) *Adenosine Proton Assignments.* The two adenosine H-8 resonances are superimposed in the 12-mer duplex state but exhibit a chemical shift difference in the strand state (Figure 8). We are unable to distinguish between dA·dT base pairs 5 and 6 for these two adenosine H-8 resonances.

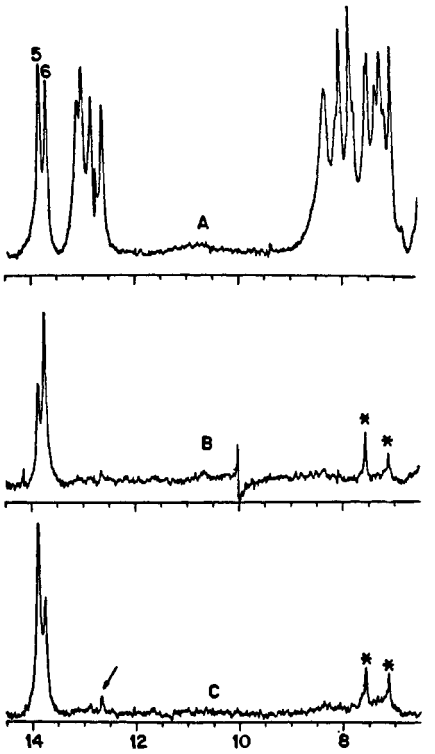

FIGURE 9: Nuclear Overhauser effect between the thymidine H-3 imino exchangeable proton and the adenosine H-2 nonexchangeable proton in the dA·dT base pairs of the 12-mer duplex in 0.1 M phosphate, 1 mM EDTA, and 4:1 $H_2O/^2H_2O$, pH 5.8, at 1 °C. (A) The decoupling pulse is applied in a resonance-free region. (B) The decoupling pulse is applied at the dA·dT base pair 6 imino proton, and the difference spectrum shows negative NOE's at the adenosine H-2 protons (see asterisks). (C) The decoupling pulse is applied at the dA·dT base pair 5 imino proton, and the difference spectrum shows negative NOE's at the adenosine H-2 protons (see asterisks) and the imino proton of dG·dC base pair 4 (see arrow). The spectra were recorded by using a Redfield 214 low-power pulse sequence. The decoupler was on for 1 s with a 10-ms delay between pulses. The signal to noise of the spectrum was improved by applying a 5-Hz line broadening contribution. A smoothing routine was applied to remove the curvature in the base line associated with the 214 pulse sequence.

Sanchez et al. (1980) demonstrated a nuclear Overhauser effect (NOE) between the nonexchangeable adenosine H-2 proton and the exchangeable uridine H-3 proton of the same A·U base pair in tRNA. It should therefore be possible to correlate the known thymidine H-3 assignments at base pairs 5 and 6 in the 12-mer duplex to their adenosine H-2 counterparts by NOE measurements.

The two thymidine imino protons in the 12-mer duplex are separated by 0.1 ppm (Figure 9A), and, hence, it is not possible to saturate one of them without partially saturating the other. Full saturation of the upfield thymidine imino proton of dA·dT base pair 6 along with partial saturation of its dA·dT base pair 5 downfield counterpart results in the observation of two resonances in the aromatic region (7.0–9.0 ppm) of the 12-mer difference spectrum at 1 °C (Figure 9B). We assign the downfield adenosine H-2 at 7.6 ppm, which exhibits the greater intensity in the difference spectrum (Figure 9B), to base pair 6 while its upfield counterpart at 7.2 ppm is assigned to base pair 5 in the 12-mer duplex (Table III).

The reverse experiment involving full saturation of the downfield thymidine imino proton of base pair 5 and partial saturation of the upfield thymidine imino proton of base pair 6 is presented in Figure 9C. The two adenosine H-2 resonances in the difference spectrum of the 12-mer at 1 °C have similar intensities (Figure 9C). This suggests that the magnitude of the thymidine H-3–adenosine H-2 NOE at dA·dT

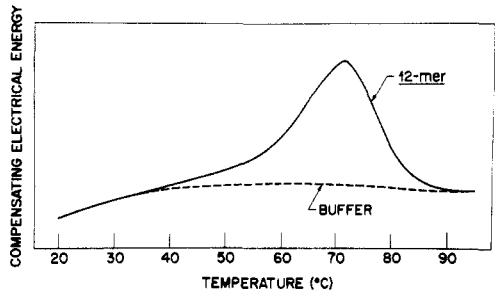

FIGURE 10: Tracing of recorder output from differential scanning calorimeter for the 12-mer in 10 mM phosphate buffer, 0.1 M NaCl, and 0.1 mM EDTA at pH 7.0. The strand concentration is 0.65 mM. The *y* axis is compensating electrical energy required to maintain the sample cell at the same temperature as the reference cell and the *x* axis is temperature.

Table V: Transition Enthalpies for the 12-mer Duplex in NaCl Solution[a]

method of analysis	0.01 M NaCl	0.1 M NaCl
calorimetric	90 kcal (mol of duplex)$^{-1}$	102 kcal (mol of duplex)$^{-1}$
van't Hoff	94 kcal ("mol")$^{-1}$	74 kcal ("mol")$^{-1}$

[a] Buffer: 10 mM phosphate and 0.1 mM EDTA, pH 7.0. Calorimetric data represent averages of at least three independent determinations.

base pair 6 is larger than that at dA·dT base pair 5 in the 12-mer duplex in solution.

Recent studies have demonstrated small NOE effects between imino protons on adjacent base pairs in tRNA (Redfield et al., 1981). Inspection of the difference spectrum in Figure 9C indicates that saturation of the thymidine imino proton of dA·dT base pair 5 results in a small negative NOE at the imino proton of dG·dC base pair 4 (indicated by arrow).

(N) Premelting Chemical Shift Changes. We observe temperature-dependent chemical shift changes at the upfield thymidine H-6 and adenosine H-2 protons (Figure 8) of the d(CGCGAATTCGCG) duplex between 0 and 60 °C. By contrast, the nonexchangeable cytidine H-5 and H-6 and guanosine H-8 resonances of the four dG·dC base pairs in the dodecanucleotide duplex do not exhibit any significant chemical shift changes in the premelting transition region (Figure 7).

Calorimetry. Figure 10 shows a tracing of the recorder output from the differential scanning calorimeter (DSC) for the thermally induced transition of the 12-mer duplex. The derived calorimetric heat capacity curves for the helix to coil transition of the dodecanucleotide duplex in 0.01 and 0.1 M NaCl are shown in Figure 11. The transition midpoints are 65.6 °C in 0.01 M NaCl and 71.3 °C in 0.1 M NaCl.

(A) Calorimetric Enthalpy. From the areas under the heat capacity curves (Figure 11), calorimetric enthalpies of 90 kcal (mol of double strand)$^{-1}$ in 0.01 M NaCl and 102 kcal (mol of double strand)$^{-1}$ in 0.1 M NaCl are obtained for the order–disorder transition of the 12-mer duplex (Table V).

(B) van't Hoff Enthalpy. Analysis of the shapes of the calorimetric heat capacity curves allows calculation of the van't Hoff enthalpy change according to the equation (Gralla & Crothers, 1973)

$$\Delta H_{\text{V.H.}} = \frac{-4.37}{(1/T_{1/2}) - (1/T_{3/4})} \quad (1)$$

This treatment yields transition enthalpies of 94 kcal in 0.01 M NaCl and 74 kcal in 0.1 M NaCl. Inspection of the data in Table V reveals that in 0.01 M NaCl the model-dependent van't Hoff and model-independent calorimetric transition

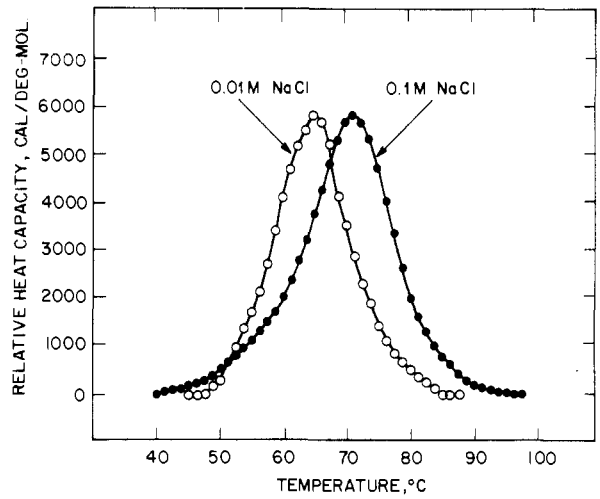

FIGURE 11: Calorimetric heat capacity vs. temperature curves for the 12-mer duplex in 0.01 and 0.1 M NaCl, 10 mM phosphate, and 0.1 mM EDTA at pH 7.0. The strand concentration is 0.65 mM.

enthalpies are equal within experimental uncertainty. This contrasts with the 0.1 M NaCl data where the van't Hoff transition enthalpy is substantially smaller than the calorimetrically determined value. The significance of the equality and inequality of the calorimetric and van't Hoff enthalpies will be discussed.

Discussion

Symmetry in the Duplex State. We observe six exchangeable imino resonances for the self-complementary d(CGCGAATTCGCG) sequence in 0.1 M phosphate, pH 7.5, at −5 °C (Figure 1), consistent with the formation of a twelve base-paired dodecanucleotide duplex with 2-fold symmetry in solution. These observations contrast with the absence of 2-fold symmetry in the d(CGCGAATTCGCG) duplex in the crystalline state (Wing et al., 1980; Drew et al., 1981; Dickerson & Drew, 1981). This difference may reflect the effect of crystal packing forces since adjacent dodecanucleotide duplexes are staggered relative to each other with hydrogen bonding between trinucleotide ends in the crystalline state (Wing et al., 1980; Drew et al., 1981; Dickerson & Drew, 1981).

Resonance Assignments. The assignment of all six resolved imino protons in the 12-mer spectrum (Table I) yields NMR markers at individual base pairs in the duplex.

We are unable to assign any of the phosphodiester resonances in the ^{31}P spectra of d(CGCGAATTCGCG) in the duplex (31.5 °C) or the strand (73.0 °C) states (Figure 5). The chemical shift dispersion is larger in the duplex state (0.45 ppm) compared to the strand state (0.25 ppm). This observation suggests variation in the O–P torsion angles and/or O–P–O bond angles of individual phosphodiester residues (Patel, 1976; Gorenstein & Kar, 1977; Simpson & Shindo, 1980) in the duplex state.

The application of spin decoupling, NOE effects, chemical modification, and comparison with suitable models has permitted the assignment of the majority of the purine H-2 and pyrimidine H-6, H-5, and CH_3-5 resonances to specific positions in the d(CGCGAATTCGCG) sequence (Tables III and IV). By contrast, we are unable to differentiate between the four guanosine H-8 and between the two adenosine H-8 protons nor can we assign any of the sugar H-1′ protons.

Fraying. We have previously demonstrated base and phosphate catalysis of the temperature-dependent exchange of the imino protons at dA·dT base pairs at the ends of the d(ATGCAT) duplex (Patel, 1974; Patel & Hilbers, 1975;

Hilbers & Patel, 1975). The sequential broadening of the thymidine imino protons with temperature in the premelting transition region was assigned to fraying at the terminal and internal dA·dT base pairs of the hexanucleotide duplex. By contrast, proton NMR studies on a pentanucleotide complementary duplex containing dA·dT base pair flanked by dG·dC dinucleotide segments provided no evidence for fraying at the dG·dC ends of the duplex (Crothers et al., 1973).

We therefore set out to probe for fraying at the dG·dC tetranucleotide ends in the d(CGCGAATTCGCG) duplex by monitoring the imino protons as a function of pH and temperature in phosphate solution. The sequential nature of the broadening with increasing temperature in the premelting region of three guanosine imino protons followed by the simultaneous broadening of the remaining guanosine and thymidine imino protons demonstrates fraying at the terminal dG·dC base pair 1, which extends up to base pair 3 for the dodecanucleotide duplex in 0.1 M phosphate at pH 7.5 (Figures 1 and 2).

Fraying is represented by a rapid equilibrium between base-paired and open states with exchange occurring through occassional leakage from the open state to solvent. Since this exchange process can be catalyzed by base, the fraying process can be identified in the premelting transition region from the pH dependence of the imino proton line widths of oligonucleotide duplexes (Patel & Hilbers, 1975). The base catalysis of the guanosine imino proton exchange rates in the 12-mer duplex is readily observable by the increase in line widths on raising the pH from 7.5 to 9.3 (Figure 4).

We also note an ~100-Hz broadening of the imino protons of base pairs 2 and 3 at 26 and 51 °C, respectively, for the 12-mer duplex in 0.1 M phosphate, pH 9.3, solution. By contrast, the duplex to strand transition of the dodecanucleotide monitored by the nonexchangeable protons exhibits a transition midpoint of 72.5 °C. These data are consistent with solvent exchange at base pairs 1, 2, and 3 occurring at temperatures below the midpoint of the cooperative component of the transition.

Premelting Transition. The large temperature-dependent chemical shifts of the thymdine imino protons of the dA·dT base pairs in the center of the duplex contrasts strongly with the small temperature-dependent chemical shifts of the guanosine imino protons of dG·dC base pairs at either end of the dodecanucleotide duplex in the premelting transition region (Figure 3).

We observe an ~0.4 ppm upfield chemical shift at the imino protons of the tetranucleotide core of the dodecanucleotide duplex over a 70 °C temperature range (Figure 3). This observation may reflect sequence-dependent conformational changes such as base-pair propeller twisting and/or duplex unwinding at the dA·dT base pairs in the premelting region.

Melting Transition. We observe upfield shifts at the dG·dC base resonances (Table III, Figure 7) and the dA·dT base resonances (Table IV, Figure 8) on d(CGCGAATTCGCG) duplex formation. These upfield shifts reflect the ring current and heteroatom magnetic anisotropy contributions (Prado et al., 1981) at a given base-pair proton from adjacent stacked base pairs in the dodecanucleotide duplex. The calculated shifts have been computed for the conformation of the dodecanucleotide in the crystalline state (Drew et al., 1981) and are reported elsewhere (B. J. Waganor, C. K. Mitra, M. H. Sarma, R. H. Sarma, and D. J. Patel, unpublished results).

The observation of a common transition midpoint of 72 ± 2 °C for the nonexchangeable protons on dG·dC base pairs 2, 3, and 4 (Table III) and dA·dT base pair 5 and 6 (Table IV) in the d(CGCGAATTCGCG) duplex in 0.1 M phosphate requires that the nonterminal base pairs of the dodecanucleotide melt cooperatively through the duplex to strand transition.

Overall Stability. From the calorimetric heat capacity curves, we obtain melting temperatures of 65.6 (0.01 M NaCl) and 71.3 °C (0.1 M NaCl) for the cooperative double to single strand transitions of the 12-mer duplex. Inspection of the 12-mer NMR melting temperature data in 0.1 M phosphate (Tables III and IV) reveals a common transition midpoint of 72 ± 2 °C for the nonexchangeable, nonterminal protons. Thus, at comparable duplex and salt concentrations NMR and DSC provide equivalent means for determining T_m values for the cooperative transition investigated in this study.

Nature of the Transition. Comparison of the van't Hoff and calorimetric enthalpies provides unique insights into the nature of the transition. If the van't Hoff enthalpy (which is calculated here assuming two-state behavior) equals the directly measured calorimetric enthalpy, then the transition occurs in an all-or-none manner. However, if "intermediate states" are significantly populated, then $\Delta H_{V.H.} < \Delta H_{cal}$ (Tsong et al., 1970). In the event of intermolecular effects (e.g., aggregation), it is possible for $\Delta H_{V.H.} > \Delta H_{cal}$. However, for several reasons we do not believe that our data are influenced by such intermolecular phenomena. To begin with, our transitions start at temperatures well above the range in which NMR line width data suggest aggregation to be significant. Furthermore, repeat calorimetric scans yield identical results thereby eliminating the possibility of effects due to aggregates whose formation is kinetically linked. For these reasons we feel that our calorimetric results correspond exclusively to the duplex to single strand transition.

Inspection of the data in Table V reveals that in 0.01 M NaCl the calculated van't Hoff enthalpy (94 kcal) is similar in magnitude to the calorimetric value [90 kcal (mol of duplex)$^{-1}$] while in 0.1 M NaCl the van't Hoff enthalpy (74 kcal) is considerably smaller in magnitude than that measured calorimetrically [102 kcal (mol of duplex)$^{-1}$]. Thus, we conclude that in 0.01 M NaCl the helix–coil transition of the dodecamer duplex approaches two-state behavior while in 0.1 M NaCl the transition does *not* occur in a two-state manner.

The detailed nature of the transitions can be further defined by using the thermodynamic data to calculate the fraction of the duplex that melts in a cooperative manner. By dividing the van't Hoff enthalpy by the calorimetric enthalpy, we obtain a measure of the size of the cooperative unit. Using the data listed in Table V, we calculate that in 0.01 M NaCl the cooperative unit involves 100% of the base pairs formed under these conditions. By contrast, in 0.1 M NaCl we calculate that the cooperative unit involves 72% of the duplex or about 9 ± 1 out of the 12 base pairs.

Acknowledgments

We are extremely grateful to Dr. Horace Drew and Professor R. E. Dickerson of Caltech for extensive discussions, for information prior to publication, and for providing the bromocytidine analogues of the 12-mer duplex. The 360-MHz correlation spectra were recorded at the Mid Atlantic Regional Facility at the University of Pennsylvania Medical School (funded by National Institutes of Health Grant RR542) and the 500-MHz Fourier transform spectra were recorded at the Cal Tech Facility (funded by National Science Foundation Grant CHE-7916324). We thank T. Perkins, U. Banerjee, and Dr. M. Croasman for recording the 500-MHz spectra. NOE studies on the 12-mer in H_2O were recorded with the University of California, Davis, Nicolet 360-MHz spectrom-

eter. We thank Drs. J. Dallas and T. Jackson for assistance and timely suggestions.

References

Albergo, D., Marky, L., Breslauer, K., & Turner, D. (1981) *Biochemistry 20*, 1409–1413.

Breslauer, K. J., Sturtevant, J. M., & Tinoco, I., Jr. (1975) *J. Mol. Biol. 99*, 549–565.

Cross, A. D., & Crothers, D. M. (1971) *Biochemistry 10*, 4015–4023.

Crothers, D. M., Hilbers, C. W., & Shulman, R. G. (1973) *Proc. Natl. Acad. Sci. U.S.A. 70*, 2899–2901.

Dickerson, R. E., & Drew, H. (1981) *J. Mol. Biol. 149*, 761–790.

Drew, H. R., Wing, R. M., Takano, T., Broka, C., Tanaka, S., Itakura, K., & Dickerson, R. E. (1981) *Proc. Natl. Acad. Sci. U.S.A. 78*, 2179–2183.

Early, T. A., Kearns, D. R., Burd, J. F., Larson, J. E., & Wells, R. D. (1977) *Biochemistry 16*, 541–551.

Early, T. A., Kearns, D. R., Hillen, W., & Wells, R. D. (1980) *Nucleic Acids Res. 8*, 5795–5812.

Gorenstein, D. G., & Kar, D. (1977) *J. Am. Chem. Soc. 99*, 672–677.

Gralla, J., & Crothers, D. M. (1973) *J. Mol. Biol. 78*, 301–319.

Haasnoot, C. A. G., den Hartog, J. H. J., deRooij, J. F. M., van Boom, J. H., & Altona, C. (1980) *Nucleic Acids Res. 8*, 169–181.

Hilbers, C. W., & Patel, D. J. (1975) *Biochemistry 14*, 2656–2660.

Hirose, T., Crea, R., & Itakura, K. (1978) *Tetrahedron Lett. 28*, 2449–2452.

Jackson, W. M., & Brandts, J. F. (1970) *Biochemistry 9*, 2295–2301.

Kallenbach, N. R., Daniel, W. E., Jr., & Kaminker, M. A. (1976) *Biochemistry 15*, 1218–1224.

Kan, L. S., Borer, P. N., & T'so, P. O. P. (1975) *Biochemistry 14*, 4864–4869.

Marky, L. A., Canuel, L., Jones, R. A., & Breslauer, K. J. (1981) *Biophys. J. 13*, 141–149.

Miller, P. S., Cheng, D. M., Dreon, N., Jayaraman, K., Kan, L. S., Leutzinger, E. E., Pulford, S. M., & T'so, P. O. P. (1980) *Biochemistry 19*, 4688–4698.

Pardi, A., Martin, F. H., & Tinoco, I., Jr. (1981) *Biochemistry 20*, 3986–3996.

Patel, D. J. (1974) *Biochemistry 13*, 2396–2402.

Patel, D. J. (1976) *Biopolymers 15*, 533–558.

Patel, D. J. (1978) *Annu. Rev. Phys. Chem. 29*, 337–362.

Patel, D. J. (1979) *Acc. Chem. Res. 12*, 118–125.

Patel, D. J. (1980) in *Nucleic Acid Geometry and Dynamics* (Sarma, R., Ed.) pp 185–231, Pergamon Press, New York.

Patel, D. J., & Tonelli, A. E. (1974) *Biopolymers 13*, 1943–1964.

Patel, D. J., & Hilbers, C. W. (1975) *Biochemistry 14*, 2651–2656.

Patel, D. J., & Canuel, L. L. (1979) *Eur. J. Biochem. 96*, 267–276.

Prado, R. F., Giessner-Prettre C., & Pullman, B. (1981) *J. Mol. Struct.* (in press).

Redfield, A. G., Roy, S., Sanchez, V., Tropp, J., & Figueroa, N. (1981) in *2nd Biomolecular Stereodynamics Conference* (Sarma, R., Ed.) pp 195–208, Academic Press, New York.

Robillard, G. T., & Reid, B. R. (1979) in *Biological Applications of Magnetic Resonance* (Shulman, R. G., Ed.) pp 45–112, Academic Press, New York.

Sanchez, V., Redfield, A. G., Johnston, P. D., & Tropp, J. (1980) *Proc. Natl. Acad. Sci. U.S.A. 77*, 5659–5662.

Schweizer, M. P. (1980) in *Magnetic Resonance in Biology* (Cohen, J. S., Ed.) Vol. 1, pp 259–302, Wiley, New York.

Selsing, E., Wells, R. D., Early, T. A., & Kearns, D. R. (1978) *Nature (London) 275*, 249–250.

Simpson, R. T., & Shindo, H. (1980) *Nucleic Acids Res. 8*, 2093–2103.

Tsong, T. Y., Hearn, R. P., Wrathall, D. P., & Sturtevant, J. M. (1970) *Biochemistry 9*, 2666–2677.

Wing, R., Drew, H., Takano, T., Broka, C., Tanaka, S., Itakura, K., & Dickerson, R. E. (1980) *Nature (London) 287*, 755–758.